Petrogenesis of the Early Cretaceous adakite-like porphyries and associated basaltic andesites in the eastern Jiangnan orogen...

Article *in* Journal of Asian Earth Sciences · November 2012

DOI: 10.1016/j.jseaes.2012.10.017

5 authors, including:

Xiao-Lei Wang
Nanjing University

Ming Tang
Rice University

R. M. Gaschnig
University of Massachusetts Lowell

Journal of Asian Earth Sciences 61 (2012) 243–256

Contents lists available at SciVerse ScienceDirect

Journal of Asian Earth Sciences

journal homepage: www.elsevier.com/locate/jseaes

Petrogenesis of the Early Cretaceous adakite-like porphyries and associated basaltic andesites in the eastern Jiangnan orogen, southern China

Xiao-Lei Wang [a,*], Xu-Jie Shu [a], Xisheng Xu [a], Ming Tang [a], Richard Gaschnig [b]

[a] State Key Laboratory for Mineral Deposits Research, Department of Earth Sciences, Nanjing University, Nanjing 210093, PR China
[b] Department of Geology, University of Maryland, MD 20742, USA

ARTICLE INFO

Article history:
Received 4 October 2011
Received in revised form 10 October 2012
Accepted 11 October 2012
Available online 23 October 2012

Keywords:
Adakite
Basaltic andesites
Early Cretaceous
Lower continental crust
EM2-type mantle
Southern China

ABSTRACT

Early Cretaceous quartz porphyries are associated with mantle-derived mafic rocks (basaltic andesites) in the eastern segment of the Neoproterozoic Jiangnan orogen, southern China. Zircons from two quartz porphyries yield identical U–Pb ages at 142 ± 1 Ma by the LA–ICP–MS method. Hornblende and augite are the dominant phenocrysts in the basaltic andesites and the groundmass plagioclase has a high anorthite content (∼80), both of which indicate high H_2O (∼6 wt.%) contents in the magma. The basaltic andesites have low TiO_2 (0.68–0.78 wt.%) and Nb/La (0.23–0.28), Nb and Ta depletions, high initial $^{87}Sr/^{86}Sr$ ratios (0.710) and unradiogenic Nd isotopes ($\varepsilon_{Nd}(t) = -3.4$ to -3.7), implying that they were generated from the partial melting of an isotopically enriched lithospheric mantle source that had been metasomatized by subduction-related fluids. The quartz porphyries (SiO_2 = 65.6–70.5 wt.%) show adakite-like geochemical features, with high Sr/Y (18.1–53.4) and La/Yb (18.6–39.4) ratios but low Y (9.44–15.2 ppm) and Yb (0.84–1.43 ppm) contents. They have low MgO (0.72–1.46 wt.%), Ni (1.04–14.7 ppm) and Cr (2.34–36.7 ppm) contents and lower Nd isotopic ratios ($\varepsilon_{Nd}(t) = -6.02$ to -7.64) than the basaltic andesites, suggesting that they may have been generated from the partial melting of the lower part of a thickened continental crust, without interaction with the (underlying) lithospheric mantle. The mafic magmas ascended from the metasomatized and hydrated lithospheric mantle and heated the lower part of thickened continental crust, triggering partial melting to form the adakite-like porphyries. The moderate levels of Sr (204–546 ppm) and negative Eu anomalies (Eu/Eu^* = 0.69–0.86) in the porphyries require the presence of minor plagioclase as residual phase in the magma source, indicating the continental crust may be not as thick (>50 km) as previously suggested. The new recognition of adakite-like porphyries and associated mafic rocks in the eastern Jiangnan orogen reveals the significant role of Neoproterozoic orogen-related crust and oceanic sediments in the formation of Mesozoic adakite-like rocks of Central-Eastern China.

1. Introduction

Adakite, which was first named by Defant and Drummond (1990) in reference to the work done by Kay (1978) on magnesian andesites from Adak Island in the Aleutians, has received great attention in the last decade (e.g., Xu et al., 2002; Chung et al., 2003; Stevenson et al., 2005; Castillo, 2006; Wang et al., 2006a; Chiaradia, 2009; Moyen, 2009; Karsli et al., 2010; Liu et al., 2010; Coldwell et al., 2011; Ling et al., 2011; Rooney et al., 2011; Sun et al., 2011; Yan et al., 2010; Zeng et al., 2011; Zellmer et al., 2012). Modern adakites mainly occur in island and continental arc settings, and their petrogenesis is generally accepted to be related to the partial melting of young and hot subducted oceanic slabs at convergent plate margins (Defant and Drummond, 1990; Castillo, 2006; Moyen, 2009; Zellmer et al., 2012). These rocks have distinct geochemical features, namely $SiO_2 \geqslant 56$ wt.%, $Al_2O_3 \geqslant 15$ wt.%, $K_2O/Na_2O \leqslant 0.5$, Sr > 400 ppm, Yb $\leqslant$ 1.8 ppm, and the absence of Eu anomalies (Defant and Drummond, 1990; Drummond et al., 1996; Martin, 1999), requiring the slab melting under pressures high enough to stabilize garnet ± amphibole and suppress the formation of plagioclase (e.g., Kay, 1978; Defant and Drummond, 1990; Rapp et al., 1991; Peacock et al., 1994; Drummond et al., 1996; Martin, 1999). Later, many intra-continental igneous rocks were considered to be "adakites" because they clearly fall within the adakite field on commonly used Sr/Y versus Y and La/Yb versus Yb discrimination diagrams. However, most of these rocks have higher K_2O contents than typical adakites. In order to reconcile the geochemical conflict, several possible mechanisms have been proposed for the genesis of intra-continental K-rich adakitic rocks: high-pressure crystal fractionation and crustal contamination of basaltic magmas (e.g., Prouteau et al., 2001; Macpherson et al., 2006), melting of hydrous garnet

* Corresponding author. Tel.: +86 25 83686336; fax: +86 25 83686016.
E-mail address: xlwangnju@yahoo.com.cn (X.-L. Wang).

1367-9120/$ - see front matter © 2012 Elsevier Ltd. All rights reserved.
http://dx.doi.org/10.1016/j.jseaes.2012.10.017

peridotite (Stern and Killian, 1996; Huang et al., 2008; Xu et al., 2008), partial melting of delaminated lowermost crust with a subsequent interaction of the melts with surrounding mantle peridotite during upward migration (e.g., Xu et al., 2002; Wang et al., 2006a; Seghedi et al., 2007), partial melting of thickened lower continental crust (e.g., Atherton and Petford, 1993; Hou et al., 2004), and mixing between basaltic and felsic magmas (Guo et al., 2007). Understanding the petrogenesis of rocks with adakite-like geochemical signatures is important in understanding Archean crustal evolution due to their similarity to Archean TTGs, the tectono-magmatic evolution at convergent margins or intra-continent areas and the potential correlation with giant porphyry-type deposits (e.g., Wang et al., 2006a; Chiaradia, 2009; Sun et al., 2011).

Intra-continental adakite-like rocks are developed in Eastern China, mainly occurring in four major locations: northeastern North China Craton, Dabie–Sulu (Jiaodong) orogenic belt, Lower Yangtze River Belt (LYRB), and Dexing area of northeastern Jiangxi Province. The latter three areas are relatively close to one another (Fig. 1a), and have received more attention. Notable geochemical differences have been described between the adakite-like rocks in the Dabie area and in the lower Yangtze River belt (LYRB), as well as the adjacent areas along the Tan–Lu Fault. The adakite-like rocks from the Dabie area lack associated Cu–Au mineralization and were interpreted to be products of the partial melting of thickened lower continental crust (e.g., Liu et al., 2010; Ling et al., 2011; Xu et al., 2012), whereas the adakite-like rocks from the LYRB are commonly associated with Cu–Au mineralization and have been considered as result of partial melting associated with mid-ocean ridge subduction (Sun et al., 2010, 2011; Ling et al., 2009, 2011). Other authors have suggested that the Early Cretaceous adakite-like rocks in the LYRB formed in a transition setting from compressional to extensional regime due to lithospheric thinning (Zhang et al., 2011) or back-arc extension (Xie et al., 2011) related to subduction of the paleo-Pacific Plate. The adakite-like rocks in the Dexing area, which host the greatest porphyry copper mineralization in Eastern China, have been the focus of similar discussions on the influence of the westward subduction of paleo-Pacific Plate. The adakite-like rocks in this area formed in the Middle Jurassic (~171 Ma) and have been proposed to be the product of partial melting of delaminated lower continental crust, although the possibility of partial melting of a Neoproterozoic relict oceanic slab has not been effectively precluded (Wang et al., 2006a). However, Zhou et al. (2012) argued that the Dexing adakite-like rocks may have been generated from the partial melting of a subducted slab with subsequent interaction with the lithospheric mantle since their geochemistry and Pb isotopic compositions cannot be explained with the delamination model. The study of any associated mantle-derived mafic rocks should provide helpful information on the geochemical characteristics of the local upper mantle and the tectonic settings in which the adakite-like rocks formed. However, no mafic rocks have so far been reported in association with the adakite-like rocks in Eastern China.

The LYRB is spatially adjacent to the nearly E–W trending Neoproterozoic Jiangnan orogen that separates the Yangtze and Cathaysia blocks. Voluminous Mesozoic felsic igneous rocks, including the Dexing adakite-like porphyries, occur in the eastern segment of the Jiangnan orogen. However, the role of Neoproterozoic juvenile crust and related relict oceanic slabs in the genesis of Mesozoic adakite-like rocks still remains unclear. In this paper, we present the first case of the association of adakitic porphyries and mantle-derived mafic rocks in the eastern Jiangnan orogen of southern Anhui Province, southern China. This new case suggests that the adakite-like porphyries were directly generated from the partial melting of the lower portion of normal-thickness crust, while the associated basal-

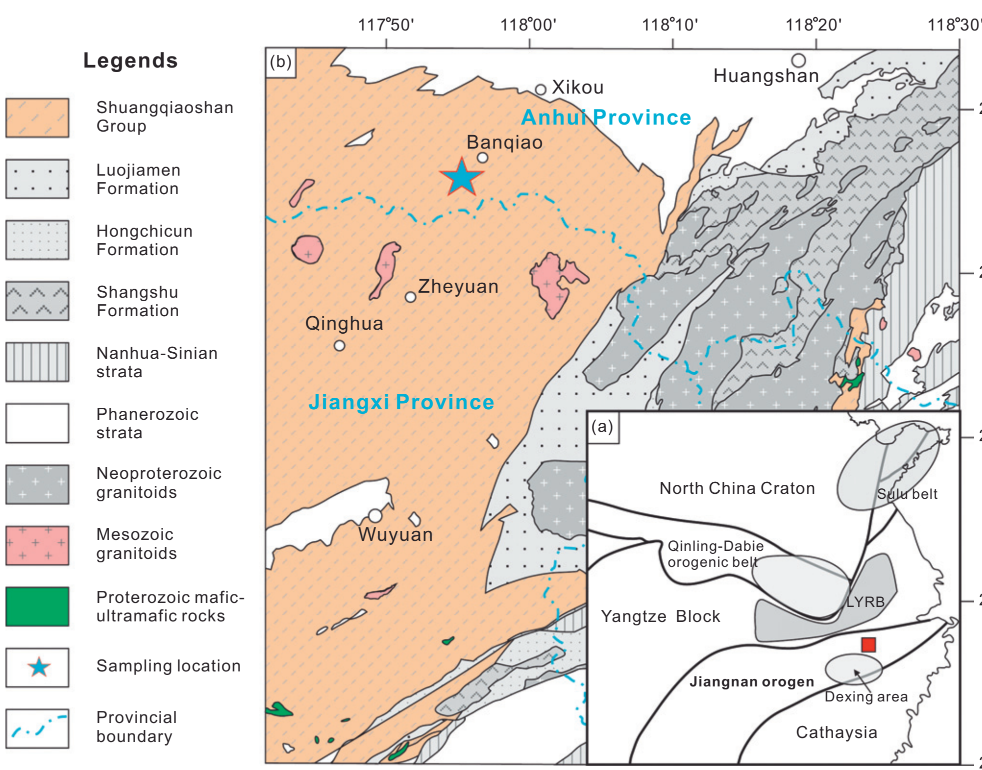

Fig. 1. Geological map of the adakite-like rocks and basaltic andesites in the eastern segment of the Jiangnan orogen. (a) Outline of the geological units of the Eastern China, with three areas for adakite-like rocks in the area: Dabie–Sulu (Jiaodong) belt, LYRB and Dexing areas. (b) Geological sketch map of the studied area (modified after JPIGS, 2007). The sampling location is indicated in figure b with red pentagon. (For interpretation of the references to color in this figure legend, the reader is referred to the web version of this article.)

tic andesites were the products of partial melting of H_2O-rich metasomatized lithospheric mantle.

2. Geological background and petrography

Central-Eastern China is a geologically complicated area, with two major ancient convergent boundaries: the Triassic Dabie–Sulu orogenic belt that separates the North China Craton (NCC) from the South China Block (SCB) (e.g. Li et al., 1999; Zheng et al., 2003), and the eastern segment of Neoproterozoic Jiangnan orogen that separates two sub-blocks (Yangtze and Cathaysia blocks) of the SCB (e.g. Wang et al., 2011) (Fig. 1a). The LYRB is located between the Dabie–Sulu orogenic belt and eastern Jiangnan orogen (Fig. 1a). Dexing adakite-like porphyries are located in the eastern Jiangnan orogen. Adakite-like rocks are widely distributed in the Central-Eastern China, with ages of ~130 Ma in the Dabie belt (Xu et al., 2012), ~124 Ma in the Jiaodong (Sulu) area (Liu et al., 2009), *ca* 138 ± 3 Ma in the LYRB (Sun et al., 2003), ~171 Ma in the Dexing area (Wang et al., 2006a; Zhou et al., 2012). Samples from this study are located in the eastern Jiangnan orogen of southern Anhui Province, about 80 km to the north of the Dexing city, just between the *ca* 970 Ma northeastern Jiangxi ophiolites and the *ca* 830 Ma southern Anhui ophiolites. The Neoproterozoic (*ca* 860–820 Ma) northwestward subduction of the Cathaysia Block resulted in the early Neoproterozoic (*ca* 970–870 Ma) arc volcanic rocks in the northwestern Zhejiang Province and back-arc basins along the southeastern margin of the Yangtze Block (i.e., the southern Anhui and northeastern Jiangxi areas in the eastern Jiangnan orogen) (e.g., Wang et al., 2011). The relict back-arc basins were filled in the late stages of the orogenic process (*ca* 860–820 Ma), with sediments from the arc-continent collisional belt to the east and the Yangtze Block to the west (Wang et al., 2007). The resulting sedimentary sequences are called the Xikou Group in the study area, and they show low-greenschist grade metamorphic features. The studied rocks are from two dykes near the Banqiao village in southern Anhui Province (Fig. 2). The widths of the two dykes are about 20 m and 40 m, respectively. They intruded (or erupted within) the Xikou Group at a very shallow level, with some metasedimentary rocks of the Xikou Group being surrounded by the quartz porphyries or trapped between the felsic and mafic igneous parts (Fig. 2a). Two mafic dykes are interlayered with felsic dykes (Fig. 2a), and the contact boundaries are not straight (Fig. 2b), suggesting that the felsic and mafic magmas were contemporaneous. The mafic rocks cut the foliation of the wall rocks, indicating that this fabric preceded the magmatism (Fig. 2c).

The studied felsic rocks are porphyritic, with phenocrysts of quartz and plagioclase. The rocks are altered to some extent, with some plagioclases generally replaced by tiny muscovite. The fresh plagioclase phenocrysts in some samples show clear oscillatory zoning (Fig. 3a). Quartz is the main mineral in the matrix of the rocks. Few quartz grains are euhedral with clear hexagonal cross sections (Fig. 3b). The mafic rocks are basaltic andesites (see the classification below), showing porphyritic texture, with phenocrysts of hornblende and clinopyroxene but not plagioclase. Hornblende generally forms long-prisms (as long as about 1 cm), and trans-twins are developed. Oscillatory zoning is also developed in these mafic minerals (Fig. DR1-a and b in Appendix). Clinopyroxenes in the basaltic andesites generally congregate together, and some of them have been replaced by chlorite. The groundmass of the basaltic andesites is mainly composed of fine-grained to cryptocrystalline plagioclase, hornblende and augite.

3. Analytical methods

All samples were prepared by crushing in an agate shatterbox. Major elements were analyzed using a VF-320 X-ray fluorescence spectrometer (XRF) at the Center of Modern Analysis, Nanjing University (NJU), following the procedures described by Franzini et al. (1972), with analytical precision better than 1%. Rare earth elements and other trace elements from the rocks were analyzed using ICP–MS (Finnigan MAT–Element 2) techniques at the State Key Laboratory for Mineral Deposits Research (MiDeR), NJU. The analytical procedures are similar to Wang et al. (2004), with precisions for most elements better than 5% (1SE). Sr–Nd isotopes were analyzed using the ID–TIMS (Finnigan MAT Triton TI) at the MiDeR–NJU. Chemical separation procedures are similar to those described by Pu et al. (2005), with average absolute standard deviation (1SE) lower than 5×10^{-6}. Mass fractionation was corrected assuming $^{86}Sr/^{88}Sr = 0.1194$ and $^{146}Nd/^{144}Nd = 0.7219$. The $\varepsilon_{Nd}(t)$ values were calculated based on the Nd isotopic compositions of $^{143}Nd/^{144}Nd$ (CHUR) = 0.512638 and $^{147}Sm/^{144}Nd$ (CHUR) = 0.1967 (Jacobsen and Wasserburg, 1980).

Major elements of minerals were determined using a JEOL JXA-8100 electron microprobe at MiDeR–NJU, following the procedures of Chen et al. (2009). All analyses were performed under an accelerating voltage of 15 kV, with a beam current of 20 nA and a beam diameter of *ca* 1 μm. Trace elements of the minerals were analyzed with an Agilent 7500a ICP–MS attached with a New Wave 213 nm ablation system at MiDeR–NJU. The diameter of laser beam is about 30 μm with a repetition of 5 Hz for hornblende and pyroxene in the basaltic rocks and *ca* 50 μm at 5 Hz for plagioclase in the quartz porphyries. NIST 610 (Pearce et al., 1997) was used as the external standard. The ^{43}Ca concentrations by electron microprobe were used as the internal standards for hornblende and pyroxene while ^{27}Al was used for plagioclase. Basaltic glass standard KL-2 (Newsom et al., 1986) was used to monitor reproducibility.

Zircons were mounted in epoxy and polished down to about half section. Transmitted and reflected light micrographs and cathodoluminescence (CL) images were used to guide the U–Th–Pb and Lu–Hf isotope analyses. CL photos were acquired with a Mono CL3+ attached to a scanning electron microscope (HITACHI S3000-N) at the Sensitive High-Resolution Ion MicroProbe (SHRIMP-II) the Beijing SHRIMP Center, Chinese Academy of Geological Sciences. LA–ICP–MS zircon U–Pb dating of this work was carried out at the State Key Laboratory of Geological Processes and Mineral Resources, China University of Geosciences (Wuhan), with an ELAN6100 attached with a 193 nm ArF-excimer laser ablation system. Spot size is 24 um for all the analyses. Detailed analytical procedures for LA–ICP–MS zircon U–Th–Pb analyzing are similar to Liu et al. (2004).

Zircon Lu–Hf analyses reported here were carried out *in situ* using a Geolas CQ 193 nm ArF excimer laser ablation system at the Institute of Geology and Geophysics, CAS. The laser ablation system is attached to a Neptune MC–ICP–MS. Both He and Ar carrier gases were used to transport the ablated samples from the laser-ablation cell via a mixing chamber to the ICP–MS torch. The analytical techniques are similar to those described in detail by Wu et al. (2006a). All analyses were carried out using a beam with a *ca* 63 μm diameter and a 5 Hz repetition rate. A new TIMS determined value of 0.5887 for $^{176}Yb/^{172}Yb$ was applied for correction (Vervoort et al., 2004). During the analytical process, we applied the mean β_{Yb} value in the same spot for the interference correction of ^{176}Yb on ^{176}Hf in order to get precise data for the individual analysis. Zircon 91500 was used as the reference standard, with a recommended $^{176}Hf/^{177}Hf$ ratio of 0.282302 ± 8 (Goolaerts et al., 2004). Decay constant for ^{176}Lu of 1.867×10^{-11} year^{-1} proposed by Söderlund et al. (2004) was adopted in this work. ε_{Hf} values were calculated according to the chondritic values of Bouvier et al. (2008).

4. Mineral geochemistry

In order to understand the magmatic evolution of the quartz porphyries and associated mantle-derived basaltic magmatism,

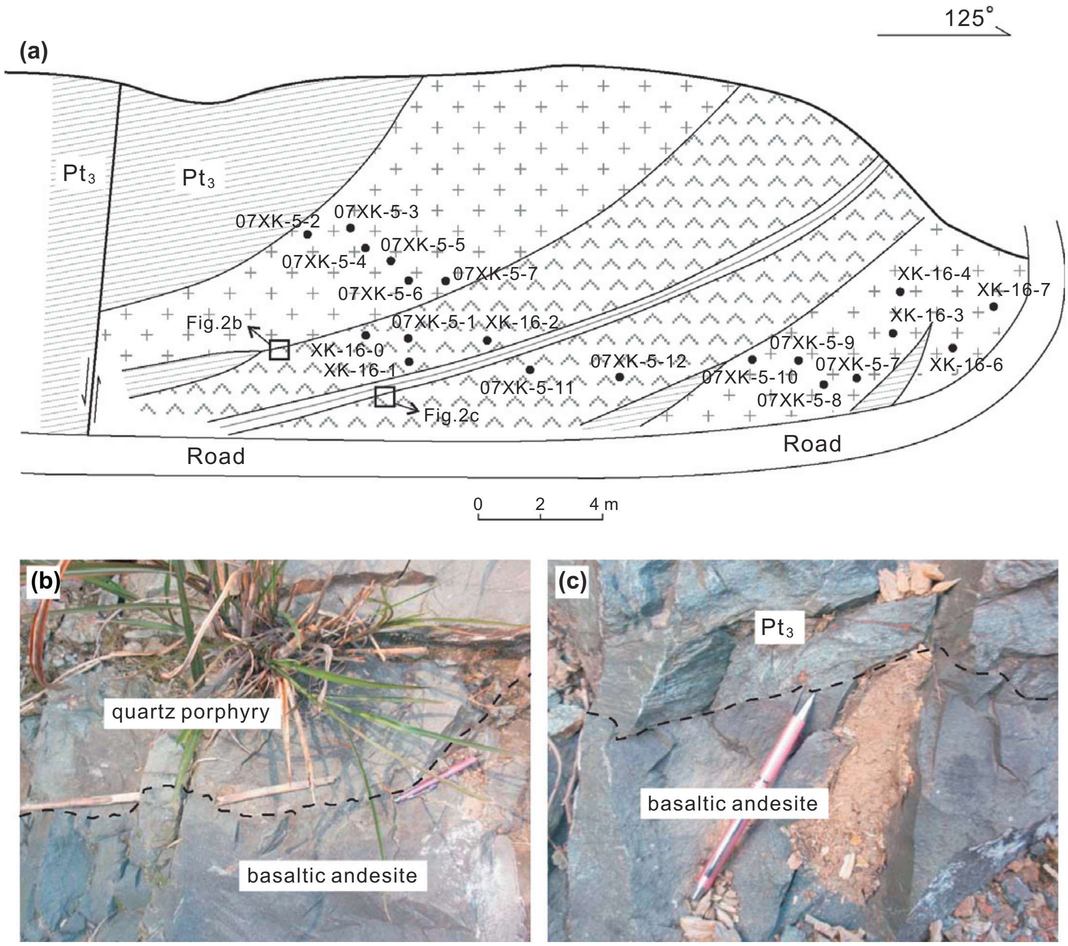

Fig. 2. Field line drawing and photos showing the geological relationships between the quartz porphyries, basaltic andesites and the wall rocks. Pt_3–Neoproterozoic sequences from the Xikou Group. The dashed lines in figure a and b indicate the contact between different rock types.

we carried out microprobe major (Tables S1 and S2 in Appendix) and LA–ICP–MS trace element (Table S3 in Appendix) analyses on hornblende, clinopyroxene and plagioclase of the basaltic andesites. Trace element analyses of plagioclase from the quartz porphyries were also obtained.

4.1. Hornblende

Hornblendes of the basaltic andesites are mostly ferri-tschermakite and ferri-potassian-tschermakite (Table S1 in Appendix). CaO contents are basically constant in hornblendes, and Mg# number range from 0.52 to 0.67. For hornblendes with zoning, the SiO_2 contents increase from core to rim (Fig. DR1 in Appendix), but Al_2O_3 and K_2O decrease (Table S1 in Appendix). The light – rare earth elements (REEs) show a backward sloping pattern, while the heavy-REE patterns are generally flat (Fig. 4a). Moderate negative Eu anomalies are present, with Eu/Eu* from 0.66 to 0.81. Sm and Nd are enriched relatively to other REEs. Zr contents in hornblendes range from 30.8 ppm to 77.2 ppm (Table S3 in Appendix), lower than the range in the whole-rock contents (121–155 ppm). The Nb contents in hornblendes (2.54–4.73 ppm) are also lower than that in the whole-rock (6.26–11.6 ppm).

4.2. Clinopyroxene

Clinopyroxenes are mainly augitic in composition (Table S2 in Appendix). TiO_2 contents are low, ranging from 0.09 to 0.59 wt.%. The highest value (0.59 wt.%) is obtained from a bright rim in a BSE image. MnO contents are high, within the range of 0.17–0.37 wt.%. Mg# numbers of the clinopyroxenes range from 0.67 to 0.84. Two types of REE patterns are evident (Fig. 4b). The first type is similar to that of hornblendes, but with lower abundances of the elements. The second type has relatively high light-REE (La–Pr) contents. The varied LREE (La–Pr) contents may result from the alteration or the LREE-enriched inclusions in the clinopyroxene. Negative Eu anomalies can also be observed in these minerals (Fig. 4b). Zr (4.13–24.3 ppm) and Nb (below detection limits) contents in the pyroxenes are even lower than those in hornblendes (Table S3 in Appendix), indicating that these two mafic minerals (especially clinopyroxene) are not the dominant mineral phases controlling the partition coefficient of Zr in the rocks.

4.3. Plagioclase

Plagioclases in the matrix generally show long prismatic shapes, indicating a rapid crystallization (Fig. DR1-c in Appendix). They have high Al_2O_3 (33.5–34.8 wt.%) and CaO (16.3–16.5 wt.%) contents, giving high An contents (from 79.9 to 81.6) (Table S2 in Appendix).

Plagioclases in the quartz porphyries are commonly phenocrysts. Trace elements were analyzed on representative plagioclase grains to test their abilities of carrying incompatible elements, in particular Sr and Eu. The contents of incompatible elements in plagioclase are generally low. Sr^{2+} can replace Ca^{2+} and thus are compatible in plagioclase. 11 analyzed plagioclase spot analyses were obtained for Sr concentrations of plagioclase. One analysis has Sr

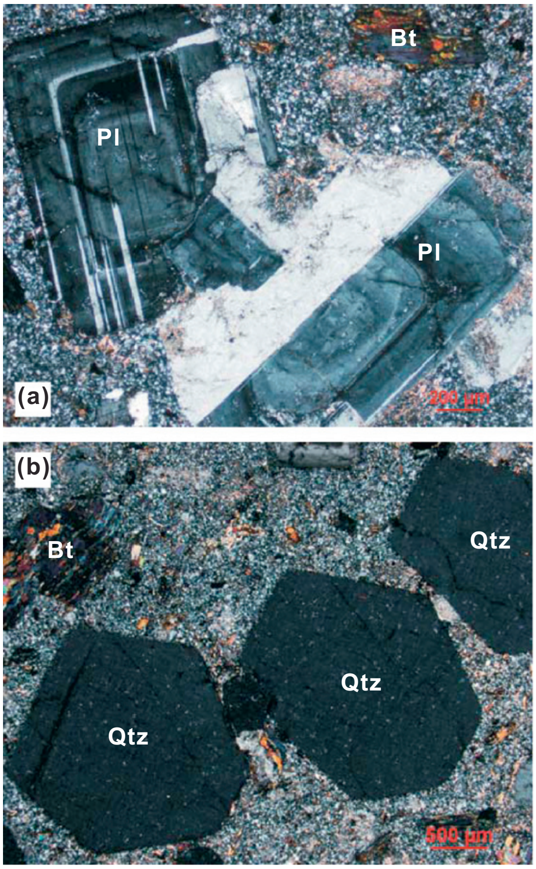

Fig. 3. Microscopic photographs of the quartz porphyries. (a) Plagioclases with zoning texture. (b) Euhedral quartz minerals.

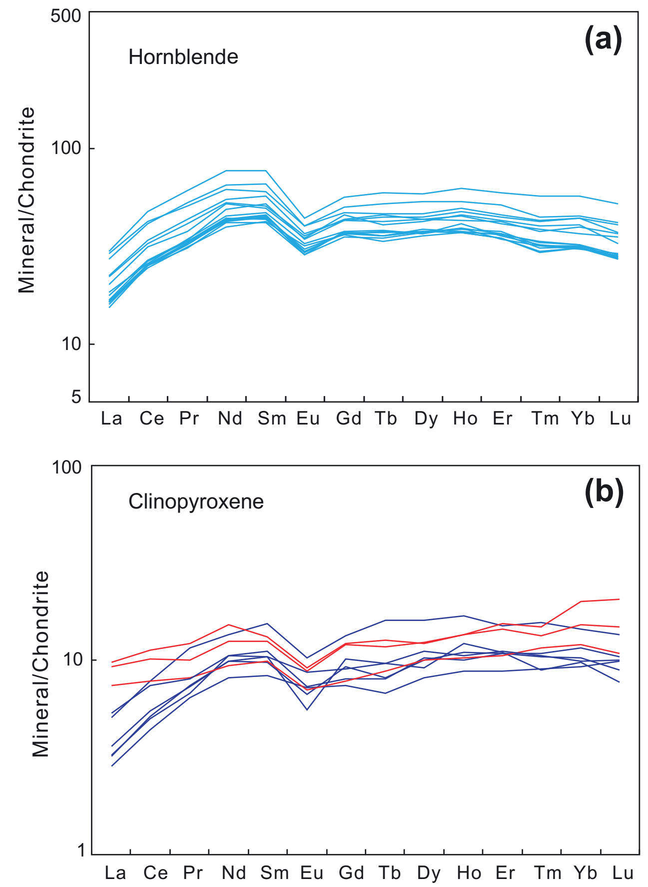

Fig. 4. Normalized REE patterns for the minerals in the basaltic andesites. The data of chondrite are from Sun and McDonough (1989). (a) Hornblende. (b) Clinopyroxene.

content at 416 ppm. The other ten analyses show Sr contents within the range 582–871 ppm (Table S4 in Appendix). Eu positive anomalies are significant in these plagioclases with Eu/Eu* = 6.3–13.0 (Table S4 in Appendix).

5. Dating results

Two porphyry samples have been dated by LA–ICP–MS (Table S5 in Appendix). CL images of zircons from the two samples show clear oscillatory zoning (Fig. DR2 in Appendix), suggesting a magmatic origin. Eighteen analyses are obtained for the sample XK-16-6. Two zircons show older ages: one is concordant with $^{206}Pb/^{238}U$ age of 833 ± 8 Ma; the other is discordant with $^{207}Pb/^{206}Pb$ age of 1040 ± 66 Ma. The remaining 16 analyses fall in one group and give an lower intercept age of 141 ± 1 Ma (MSWD = 0.57), consistent with the weighted mean $^{206}Pb/^{238}U$ age of 142 ± 1 Ma (Fig. 5a; *n* = 16, MSWD = 0.77). Th contents of these zircons range from 130 to 1277 ppm, and U within the range of 188 to 2265 ppm, giving the Th/U ratios of 0.28–0.94.

Thirteen analyses were obtained for the sample XK-17-2. Th contents of the spot analyses range from 113 to 1439 ppm, and U contents range from 176 to 4599 ppm, giving the Th/U contents of 0.29–0.92 (Table S5 in Appendix). The weighted mean $^{206}Pb/^{238}U$ age is 142 ± 1 Ma (Fig. 5b; *n* = 13, MSWD = 1.5).

6. Geochemistry

The mafic rocks of this study have SiO_2 contents of 53.1–55.1 wt.% (Table S6 in Appendix), falling in the basaltic andesite field in the SiO_2–alkali diagram (Fig. 6a). They have low TiO_2 (0.68–0.77 wt.%) and high Al_2O_3 contents (14.9–16.3 wt.%). K_2O contents (2.11–3.26 wt.%) are higher than Na_2O, belonging to the high-K calc-alkaline series (Fig. 6b). Mg# values are moderately high, within the range of 54–59, apart from one sample of 51, indicating that the magma may have not experienced significant fractional crystallization, which is consistent with the absence of significant correlations between major and incompatible element ratios versus SiO_2 (Fig. 7). Light rare earth elements are enriched relative to the heavy REEs (Fig. 8a), with $(La/Yb)_N$ = 4.3–4.6. HREEs are not internally fractionated, with $(Dy/Yb)_N$ = 0.85–0.94. Weak negative Eu anomalies are observed (Eu/Eu* = 0.72–0.79). Negative anomalies of Nb, Ta, Ti and Ba are observed for the basaltic andesites in normalized trace element patterns (Fig. 8b), but Zr and Hf anomalies are not evident.

The quartz porphyries have varied SiO_2 contents (65.6–70.5 wt.%), falling in the dacite field in the SiO_2–alkali diagram (Fig. 6a). They have high alkali contents, and the K_2O contents are generally equal to Na_2O (apart from one sample with Na_2O content of 6.1 wt.%), resulting in the K_2O/Na_2O ratios of about 1.0. These rocks can also be classified as high-K calc-alkaline series (Fig. 6b). The aluminum saturation index (ASI) is generally within the range 1.01–1.15, apart from one sample of 1.43 (Table S6 in Appendix). MgO contents vary from 0.72 to 1.46 wt.%, and the calculated Mg# numbers range from 39 to 46. Weak negative correlations can be observed in the Harker diagrams of TiO_2, FeO^t, K_2O, MgO, CaO, Eu/Eu*, La/Yb and Sr/Y versus SiO_2 (Fig. 7), indicating the magmatic crystallization differentiation. Sr contents range from 201 to 546 ppm, which is a bit lower than typical adakites. However, Y (9.44–12.0 ppm, except one sample of 15.2 ppm) and Yb (0.84–1.03 ppm, except one of 1.43 ppm) contents (Table S6

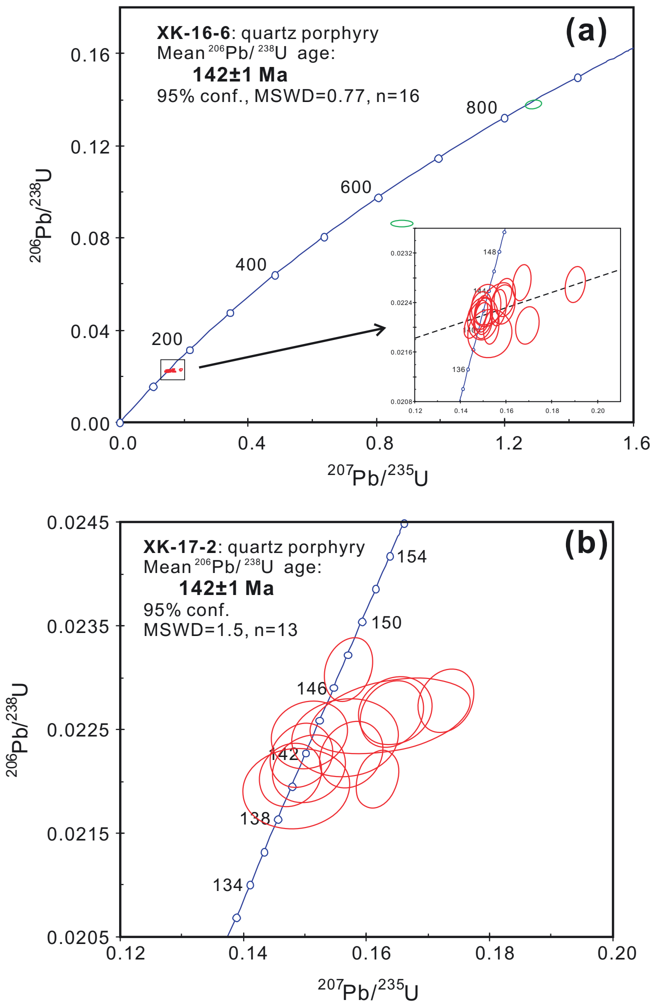

Fig. 5. Zircon U–Pb Concordia for the quartz porphyries.

in Appendix) are both within the ranges for typical adakites (Defant and Drummond, 1990). The adakite-like geochemical features are evidenced in their fractionated REE patterns (Fig. 8c), with a mean $(La/Yb)_N$ of 23.4, except one sample of 13.4. These rocks have clear depletions in Nb, Ta and Ti and moderate depletions in Sr and Ba (Fig. 8d). The high Sr/Y and La/Yb but low Y and Yb lead the quartz porphyries to plot in the adakite field in the discrimination diagrams (Fig. 9a and b).

Both the studied mafic and felsic rocks have evolved Nd and Sr isotopic compositions (Table S7 in Appendix). The basaltic andesites have relatively higher $\varepsilon_{Nd}(t)$ (−3.37 to −3.74) and lower initial $^{87}Sr/^{86}Sr$ ratios (0.710), while the $\varepsilon_{Nd}(t)$ and initial $^{87}Sr/^{86}Sr$ of the porphyries range from −6.02 to −7.64 and 0.712–0.714 respectively. The whole-rock single-stage (T_{DM1}) and two-stage (T_{DM2}) Nd model ages fall within the ranges of 1262–1591 Ma and 1422–1554 Ma respectively (Table S7 in Appendix). The dated zircons from the two porphyries (XK-16-6 and XK-17-2) have similar Hf isotopic compositions (Table S8 in Appendix), both displaying normal distribution (Fig. 10), yielding mean $\varepsilon_{Hf}(t)$ of -4.3 ± 0.5 (n = 16, MSWD = 3.9) and -4.6 ± 0.6 (n = 14, MSWD = 5.4), respectively. Two-stage (T_{DM2}) Hf model ages for the dated zircons from the two adakite-like quartz porphyries yield mean values of 1442 ± 33 Ma (n = 16, MSWD = 9.8) and 1461 ± 36 (n = 14, MSWD = 14) (Fig. 10), which are consistent with the T_{DM2} whole-rock Nd model ages for the two samples (1554 Ma for XK-16-6 and 1422 Ma for XK-17-2; Table S7 in Appendix) and are more homogeneous, suggesting that their Nd–Hf isotopes are basically coupled and the Hf isotopes are better to trace their source features.

7. Discussion

7.1. Melting of the enriched lithospheric mantle

As the first case of the association of mafic rocks and adakite-like felsic rocks in Eastern China, it is necessary to investigate the genesis of the mafic rocks and their possible petrogenetic relationship with the felsic adakite-like rocks. Although the two rock types are closely spatially and temporally associated, there is no clear evidence for the magma mixing in the field. Hornblende is the dominant phenocryst in the mafic rocks. However, no amphibole was found in the felsic rocks and no quartz grains from the porphyries were found in the basaltic andesites. Moreover, the two rock types form widely dispersed groups in major element versus SiO_2 plots (Fig. 7), indicating that there is no evolutionary relationship between the mafic and felsic rocks. It is also supported by the differences in Nd isotopes. The adakite-like quartz porphyries have lower $\varepsilon_{Nd}(t)$ values and higher initial $^{87}Sr/^{86}Sr$ ratios, suggesting they might have been generated from the partial melting of crustal rocks. Although the mafic rocks have relatively high Mg# and low SiO_2 contents, their negative $\varepsilon_{Nd}(t)$ values and high initial $^{87}Sr/^{86}Sr$ ratios (0.710) imply that they may have been generated from an

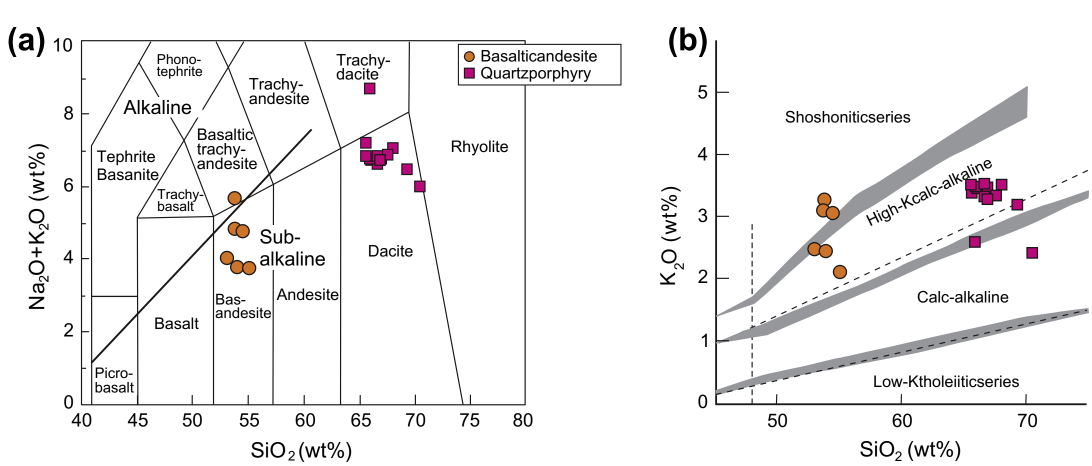

Fig. 6. Rock classification diagrams for the rocks in the studied area. (a) SiO_2–alkali diagram (after Maitre et al., 1989). (b) SiO_2–K_2O diagram (after Maitre et al., 1989).

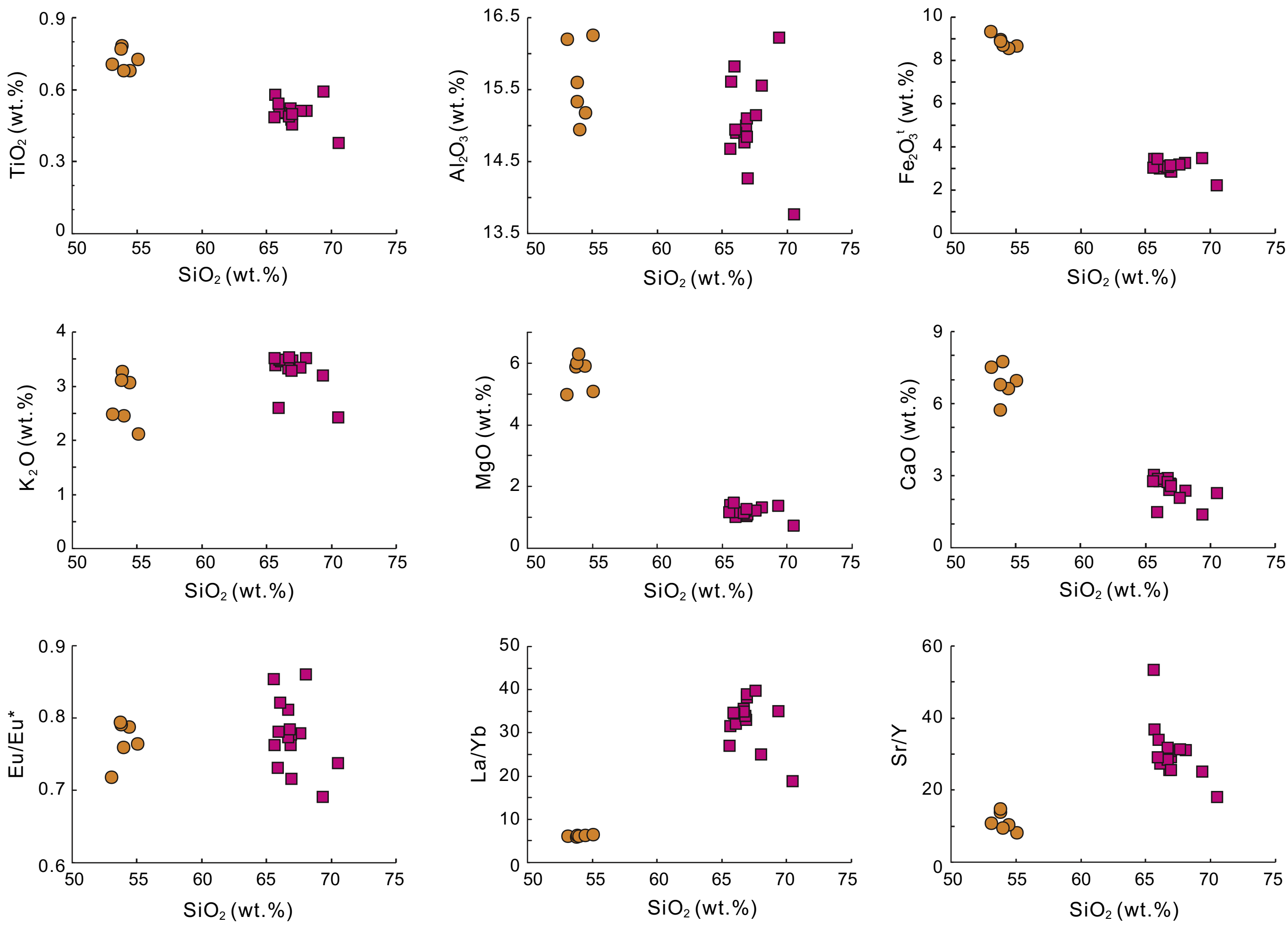

Fig. 7. Harker diagrams of the major and incompatible element ratios versus SiO_2 for the studied rocks.

enriched mantle source. This enriched isotopic feature is seen in the middle Jurassic to later Cretaceous mafic rocks in many areas of southern China, such as the eastern Nanling area (Wang et al., 2008), the ~142 Ma lamprophyre and diabase dykes in the Qianlishan area, south Hunan Province (Jiang et al., 2006), 130–132 Ma Luzong mafic volcanic rocks in the LYRB (Tang et al., 2012), and the Late Yanshannian basalts in northeastern Hunan Province (Xu et al., 2006). In addition, Zr/Nb ratios of the mafic rocks range from 20.1 to 21.2, falling within the range between continental crust and N–MORB, but higher than that of the EM1 and OIB. Nb/La ratios range from 0.23 to 0.24 and are similar to typical arc basalts. La/Ta ratios are higher than 30, indicating they may be generated from the partial melting of lithospheric mantle, rather than asthenosphere.

The absence of plagioclase phenocrysts in the mafic rocks indicates high contents of water in the magma source because the plagioclase phenocrysts are unstable in a high water pressure environment. This is also supported by the presence of hornblende phenocrysts. According to the experimental studies (Blatter et al., 2001; Moore and Carmichael, 1998), the dissolved water will be over 5.5 wt.% in the magma source when hornblende and clinopyroxene form as phenocrysts but not the plagioclase. The corresponding magma temperature is about 980–1000 °C, and the water pressure is over 2.4 kbar. Although phenocrysts of plagioclase do not exist, the matrix of the basaltic andesites is mainly composed of plagioclase. The content of anorthite (An) in this plagioclase is as high as about 80. Basalts with high-An plagioclase have been reported in arc environments (e.g., Kuno, 1960; Panjasawatwong et al., 1995; Sisson et al., 1996; Chen and Zhou, 2001) and their presence in the basaltic andesite matrix also supports the inference of a magma source with high water content, based on experimental evidence (e.g., Sisson and Grove, 1993; Panjasawatwong et al., 1995). Therefore, the basaltic andesites may be generated from the partial melting of water-rich enriched lithospheric mantle.

La/Sm and Zr/Nb ratios of the basaltic rocks are constant, indicating weak fractional crystallization. Weak negative Eu anomalies may suggest the fractional crystallization of plagioclase, which is also supported by the *in situ* REE distribution patterns of clinopyroxene and amphibole (Fig. 4). Clinopyroxene typically does not have a negative Eu anomaly and the presence of negative anomalies in the clinopyroxene grains of the studied basaltic andesites suggest that plagioclase may have formed earlier than the clinopyroxene.

Two representative samples from the basaltic andesites show initial $^{87}Sr/^{86}Sr$ ratios of 0.710, implying that the mantle source for these mafic rocks has an EM2-like geochemical feature (Fig. 11), which requires either the involvements of continental upper crust or oceanic sediments in the magma source. The significant contamination of the source with continental upper crust can be precluded because: (1) these basaltic andesites have constant La/Sm and La/Nb ratios without correlations; (2) Sr contents of these rocks are high (283–507 ppm), and is comparable to those of the quartz porphyries (Sr = 204–546 ppm), but higher than those of the wall rocks from the Shuangqiaoshan and Xikou Groups (mostly <140 ppm; our unpublished data); and (3) the initial $^{87}Sr/^{86}Sr$ of the Neoproterozoic

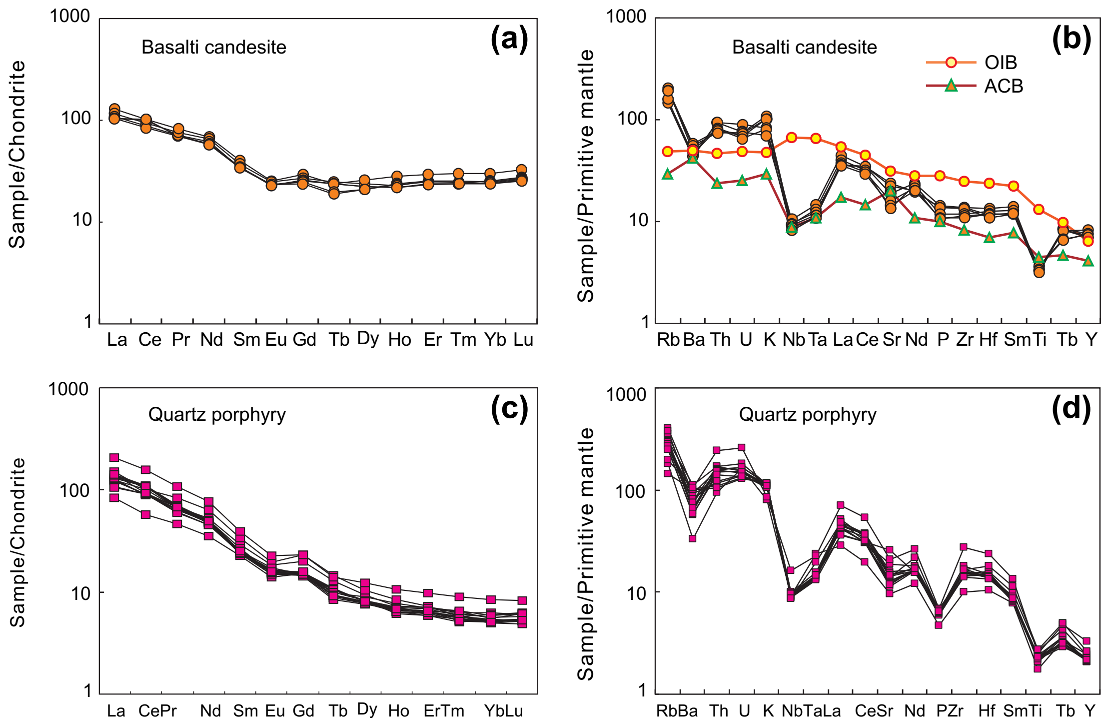

Fig. 8. Normalized REE and trace element patterns for the studied rocks. Chondrite, primitive-mantle and ocean island basalt (OIB) data are from Sun and McDonough (1989). The data for average continental-arc basalts (CABs) are from Kelemen and Hanghøj (2004).

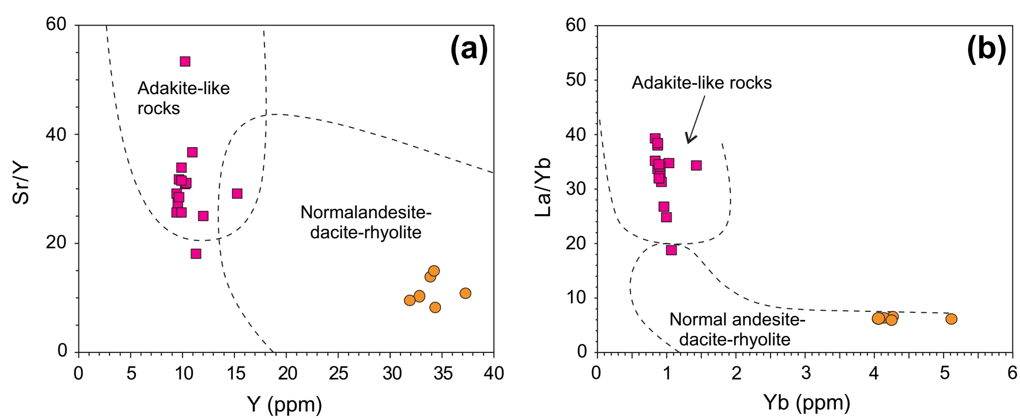

Fig. 9. Sr/Y–Y (a) and La/Yb–Yb (b) diagrams showing the quartz porphyries in southern Anhui Province have adakite-like geochemical features. The fields of adakite-like rocks and normal andesite-dacite-rhyolite are from Richards et al. (2012).

crustal rocks is 0.709–0.712 if calculated at 140 Ma, indicating that the required proportion of contaminating crustal materials would need to be at least >50%. Therefore, oceanic sediments probably have been incorporated into the source of the basaltic andesites, and this incorporation may have taken place before the Early Cretaceous.

7.2. Origin of the adakite-like porphyries

The quartz porphyries have high Sr/Y and La/Yb ratios but low Y and Yb contents (Fig. 9), resembling typical adakites defined by Defant and Drummond (1990). These adakite-like geochemical features require residual garnet and hornblende in the magma source. For typical adakites, Sr is highly incompatible in the residual mineral phases but Y is not, which may result in the high Sr/Y ratios of the adakitic melts. However, the Sr contents for the quartz porphyries (201–546 ppm) in this study are not as high as typical adakites (>400 ppm). A negative correlation is evident between Sr/Y and SiO_2 (Fig. 7), suggesting that the primary magmas for the quartz porphyries probably have higher Sr/Y ratios and Sr contents. The fractional crystallization of plagioclase is a possible mechanism for the decreasing Sr, which is supported by the weak whole-rock negative Eu anomalies (Fig. 8c) and the positive anomalies of plagioclase (Table S4 in Appendix). In particular, the Sr contents in the plagioclases are significantly higher than those of the whole-rock (Table S4 in Appendix). However, there is no correlation of Sr and Ba versus Eu/Eu*, indicating the fractionation of plagioclase may be not sufficient to explain the decreasing Sr contents. An alternative explanation is that some of the plagioclase stays in the magma source as one of the residual phases. Partial melting of crustal rocks with amphibole + plagioclase + garnet as the residual phases could lead to magmas with high SiO_2 contents but low Al_2O_3 contents (<15 wt.%) and Sr concentrations

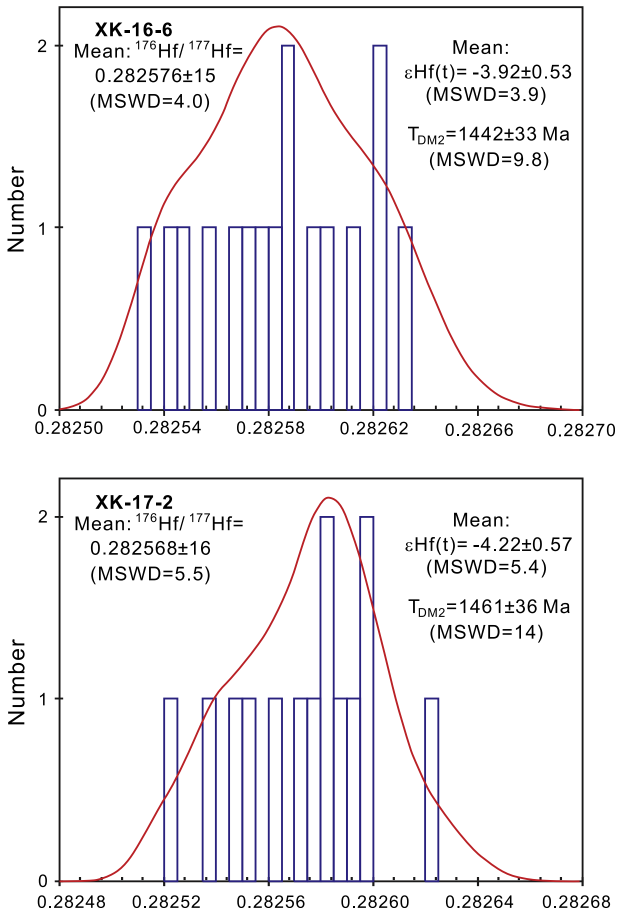

Fig. 10. Relative probability of Hf isotopes for zircons from the quartz porphyries in southern Anhui Province.

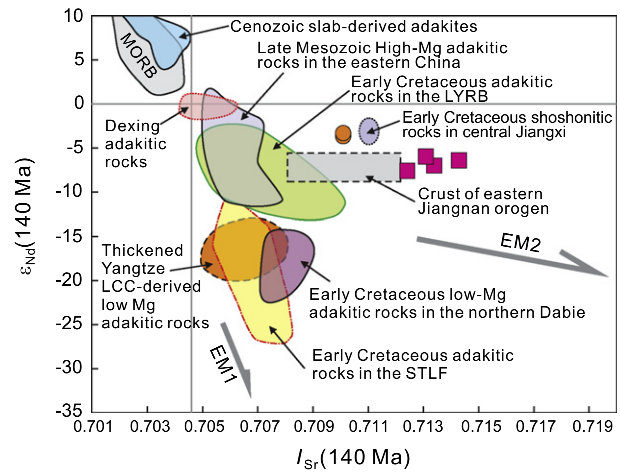

Fig. 11. Initial Sr–Nd isotopic compositions of adakite-like rocks in Central-Eastern China. EM1, enriched mantle-1; EM2, enriched mantle-2. Data sources: Cenozoic slab-derived adakites (Defant and Kepezhinskas, 2001), MORB and marine sediments (Hofmann, 2003), Early-Cretaceous adakite-like rocks in LYRB (Liu et al., 2009), Dexing adakite-like rocks (Wang et al., 2006a), Early Cretaceous adakite-like rocks in STLF (Liu et al., 2009), Early Cretaceous low-Mg adakite-like rocks in the northern Dabie (Xu et al., 2012), Thickened Yangtze LCC-derived low Mg adakitic rocks (Liu et al., 2009), Late Mezozoic high-Mg adakitic rocks in the Eastern China (Xu et al., 2012), Early Cretaceous shoshonitic rocks in central Jiangxi (Wu et al., 2011). The area for crust of eastern Jiangnan orogen is defined by the Neoproterozoic granitic rocks (Xucun, Xiuning, Shexian and Jiuling plutons) in the eastern Jiangnan orogen with data from Li et al. (2003) and Wu et al. (2006b).

(<400 ppm), as well as weak negative Eu anomalies (Defant and Drummond, 1990; Zhang et al., 2003). Typical adakites are believed to have garnet as a major residual phase, and their residual source should be eclogite, amphibole-bearing eclogite or garnet-amphibolite, in a depth greater than 40 km (>~1.2 GPa). When the garnet is the dominant residual mineral in the magma source, Y/Yb ratios of the adakitic melts are generally higher than 10 (Ge et al., 2002). The quartz porphyries of this study have Y/Yb ratios close to 10, suggesting that hornblende is the dominant residual mineral phase in the magma source and the magma source may be not as deep as for typical adakites. Moreover, their coupled Nd–Hf isotopic features preclude significant amounts of garnet as residual minerals since garnet is significantly enriched in HREE and thus its residue can lead to low Lu/Hf ratio in the melt (Vervoort et al., 2000; Wu et al., 2006b).

The adakites were originally suggested to be formed from the partial melting of subducted oceanic crust (Defant and Drummond, 1990). However, the adakite-like quartz porphyries of this study were formed in an intra-continental setting. Similarly, most of the adakite-like rocks in Eastern China generally show intra-continental settings, without definite evidence for coeval subduction (Zhang et al., 2003; Castillo, 2006). It has been commonly accepted that the Early-Cretaceous adakite-like rocks in the Dabie area formed by partial melting of (over-) thickened lower continental crust (Ling et al., 2009; Liu et al., 2009, 2010, 2011; Xiong et al., 2010; Xu et al., 2012). However, the question of the origin of the Mesozoic adakite-like rocks in the LYRB and Dexing areas has received considerable debate. Originally, partial melting of the delaminated lower continental crust was believed to be the main mechanism for the genesis of these rocks (Xu et al., 2002; Wang et al., 2006a,b). Later, based on systematic comparisons of geochemistry and mineralization of the adakites along the eastern and western margins of the Pacific Plate, melting of oceanic slabs, utilizing a ridge subduction model, was applied to the formations of adakite-like rocks and associated porphyry copper deposits in the LYRB and Dexing areas (Ling et al., 2009, 2011; Liu et al., 2010; Deng et al., 2012). Other proposed models for similar K_2O-rich adakite-like rocks include: high-pressure crystal fractionation and crustal contamination of basaltic magmas (e.g., Prouteau et al., 2001; Feeley and Hacker, 2006; Macpherson et al., 2006), mixing between basaltic and felsic magmas (Guo et al., 2007), and melting of hydrous garnet peridotite (Stern and Kilian, 1996; Xu et al., 2008). The fractional crystallization of basaltic magmas under high-pressure and partial melting of hydrous garnet peridotite both seem impossible for the studied quartz porphyries because they have high SiO_2 contents (up to 70.5%) which would require the existence of significant amounts of intermediate rocks. However, the field studies indicate that the Early Cretaceous igneous rocks in the studied area are bimodal in composition. Particularly, there is no clear correlation of elements between the adakite-like rocks and the associated mafic rocks (Fig. 7), but large compositional gaps, precluding the mixing or evolution between the studied mafic and felsic rocks. In addition, there are positive correlations of La/Sm versus La and Zr/Nb versus Zr (not shown here), indicating that partial melting, rather than fractional crystallization, may be the dominant mechanism controlling the elemental variations of the quartz porphyries.

As for the genesis of the studied adakite-like quartz porphyries in southern Anhui Province, the key is to distinguish the roles of Mesozoic oceanic slabs and lower continental crust. If the juvenile Mesozoic oceanic slabs were involved into the origins of theses rocks, more radiogenic Nd isotopic compositions would be expected. However, these adakite-like rocks have negative $\varepsilon_{Nd}(t)$ values, which would require significant subsequent incorporation of upper continental crust. This process, if happened, would erase the adakitic geochemical features (such as high Sr/Y and La/Yb ratios) since the melts from the middle-upper continental crust would not have the adakitic signatures. In addition, the associated mafic rocks also have enriched Nd isotopic characteristics, inconsistent with the melting of Mesozoic oceanic slabs. The partial melting of relicts of previously (Neoproterozoic?) subducted oceanic crust in the mantle or lower crust could generate such negative $\varepsilon_{Nd}(t)$, low Th abundances and Th/Ce ratios for the studied rocks. However, these quartz porphyries have low FeO^*/MgO ratios and Al_2O_3, MgO, Ni and Cr contents (Table S6 in Appendix; Figs. 9 and 14), suggesting that this mechanism may be not possible. For the same reasons, the melting of an enriched mantle source is also not appropriate for the genesis of the Early Cretaceous adakite-like rocks in the southern Anhui Province. Liu et al. (2010) gave a detailed comparison between the adakite-like rocks in the Dabie area and the LYRB, and suggested the ore-bearing adakite-like rocks in the LYRB were generated from the melting of oceanic slab but the ore-barren adakite-like rocks in the Dabie area from the melting of lower continental crust. The studied adakite-like rocks in the southern Anhui Province are geochemically similar to the Dabie adakite-like rocks in major and trace elements (e.g. Al_2O_3, Ni, Cr contents and K_2O/Na_2O, Sr/Y and La/Yb ratios), whereas they are close to the Sr–Nd tendency of the ore-bearing adakite-like rocks in the LYRB (Fig. 11). The partial melting of oceanic crust could not explain the bulk geochemical features and the Sr–Nd isotopic characteristics could be resulted from other mechanisms, e.g. the melting of old mafic crusts with mixing of marine sediments.

The partial melting of delaminated lower crust has been discussed greatly in recent years for the genesis of the adakite-like rocks (e.g., Xu et al., 2002; Xiong et al., 2003; Hou et al., 2004; Castillo, 2006; Wang et al., 2006a). When the crust is thickened due to orogenic processes, the lower crust can reach the eclogite stability field. The thickened lower curst may subsequently fall into the asthenospheric mantle due to its high density, and if melted due to the high surrounding temperatures, it would generate intermediate to felsic adakitic magma. The magma would mix with the melt from overlying lithospheric mantle during its ascent and develop high MgO, Ni and Cr contents. The adakite-like quartz porphyries of this study clearly do not merit this explanation due to their low Mg#, MgO, Ni and Cr (Fig. 12a–c). In an alternative model, the thickened lower crust could be melted *in situ* due to the heating of underplating basaltic magma. In this case, the generated magma would show adakite-like geochemical features (e.g., high La/Yb and low Yb and Y) without significantly high MgO, Ni and Cr contents. This mechanism is reasonable for the petrogenesis of the Early Cretaceous quartz porphyries in the eastern Jiangnan orogen, as indicated in Fig. 12. However, their magma source may be not as deep as typical adakites, as discussed above. The residual mineral association of predominantly hornblende with limited garnet and plagioclase suggests that they may have been generated at a depth of *ca* 40 km, which could not be considered as a significantly thickened lower continental crust.

Although the underplating of basaltic magmas has been suggested as a possible heat source for the partial melting of adakitic rocks in many cases, few examples of the associated basaltic rocks have been reported. The association of Early Cretaceous quartz porphyries and hornblende-rich basaltic andesites in the eastern Jiangnan orogen is the first reported case in Central-Eastern China and thus provides a good natural lab for studying adakitic rocks in the area. If crustal thickening did occur in the Dexing area as suggested by Wang et al. (2006a), the adakite-like rocks of this study at least imply that the extent of thickening may be different between southern Anhui and northeastern Jiangxi.

In southern China, the adakite-like rocks seem to occur at boundaries between continental blocks. For example, the adakite-like rocks in the Dabie and Jiaodong areas are along the Triassic UHP Dabie–Sulu belt, and the LYRB is on the northern margin of the Yangtze Block (Liu et al., 2010). It seems that the Neoproterozoic eastern Jiangnan orogen may be another continental boundary with the occurrence of voluminous adakite-like rocks, as evidenced by the Mesozoic adakitic rocks in the Dexing area (Wang et al., 2006a, 2012), the early Neoproterozoic adakitic rocks in the ophiolites of northeastern Jiangxi Province (Li and Li, 2003; Gao et al., 2009), and the Early Cretaceous adakite-like quartz porphyries in southern Anhui Province of this study. This implies that the formation of these adakite-like rocks may have close relationships with the melting of late Mesoproterozoic to early Neoproterozoic arc-related crust and related oceanic crustal materials (ophiolites and overlying sediments) that were formed during the Neoproterozoic orogenic processes between the Yangtze and Cathaysia Blocks and finally trapped as part of the lower continental crust. The distinct Sr–Nd isotopic features of the *ca* 140 Ma adakite-like rocks in the southern Anhui Province are different from the other previously-reported adakite-like rocks in Eastern China (Fig. 11) and are close to the EM2 field, along with the associated mafic rocks (Fig. 11), implying the incorporation of Neoproterozoic oceanic sediments in the formation of these rocks. Similar Sr–Nd isotopic signatures have been reported for the Early-Cretaceous shoshonitic rocks in central Jiangxi Province (Wu et al., 2011), eastern Jiangnan orogen. Therefore, an EM2 end-member may have existed in the eastern Jiangnan orogen during Mesozoic time and contributed greatly to the genesis of some Mesozoic igneous rocks. In particular, the Sr–Nd isotopic signature of the Cretaceous adakite-like porphyries is very close to that of the eastern Jiangnan orogen, as defined by the Neoproterozoic granitic rocks (Fig. 11), suggesting that the sources of Cretaceous adakitic rocks and Neoproterozoic granitic rocks have close genetic correlations. The crustal Hf model ages (T_{DM2}) (mean values of 1442 ± 23 Ma and 1461 ± 36 Ma, respectively) are basically similar to those of magmatic zircons from the Neoproterozoic orogeny-related igneous rocks in the eastern Jiangnan Orogen (Table S8 in Appendix), and the Neoproterozoic magmatism (e.g. the Xucun, Shexian, Xiuning and Jiuling granitic plutons) in the area has been suggested to be resulted from the reworking of Late-Mesoproterozoic to Early Neoproterozoic juvenile crust rocks (Wu et al., 2006b; Zheng et al., 2008). Therefore, the magma end-member for the Early-Cretaceous adakite-like rocks is probably related to the Neoproterozoic orogenic juvenile crust and relict of oceanic sediments between the Yangtze and Cathaysia blocks. Tang et al. (2012) similarly proposed a close genetic relationship between the occurrence of subducted late Mesoproterozoic to early Neoproterozoic crustal materials and the genesis of the *ca* 130 Ma Luzong volcanic rocks in the Lower Yangtze area that have adakite-like geochemical features, suggesting the presence of widespread Neoproterozoic orogeny-related crustal materials between the Yangtze and Cathaysia Blocks.

7.3. Tectonic model

The tectonic setting of the Mesozoic intra-continental magmatism in southern China is a long-debated issue (e.g., Li et al., 2003; Li and Li, 2007; Zhou and Li, 2000; Zhou et al., 2006; Wang et al., 2006a,b, 2008; Niu, 2005). The key is to evaluate the influence of subduction of the Pacific Plate (e.g., Chen et al., 2008). Zhou and Li (2000) proposed that the roll back and the change of subduction angle was the main driver for the widespread Mesozoic magmatism in southern China. Later, they renewed this model and suggested a tectonic transition from Tethys tectonic regime to Pacific regime during *ca* 200–180 Ma that controlled the distribution of Mesozoic igneous rocks in southern China (Zhou et al., 2006). In contrast, Li and Li (2007) proposed a westward flat-subduction model related to the Pacific Plate to explain the origin of Mesozoic magmatism in this area. Sun et al. (2007, 2011) suggested there was a change in the subduction orientation of the Pacific Plate and the subduction of an ocean-ridge occurred and influenced the Lower Reaches of Yangtze River. However, less

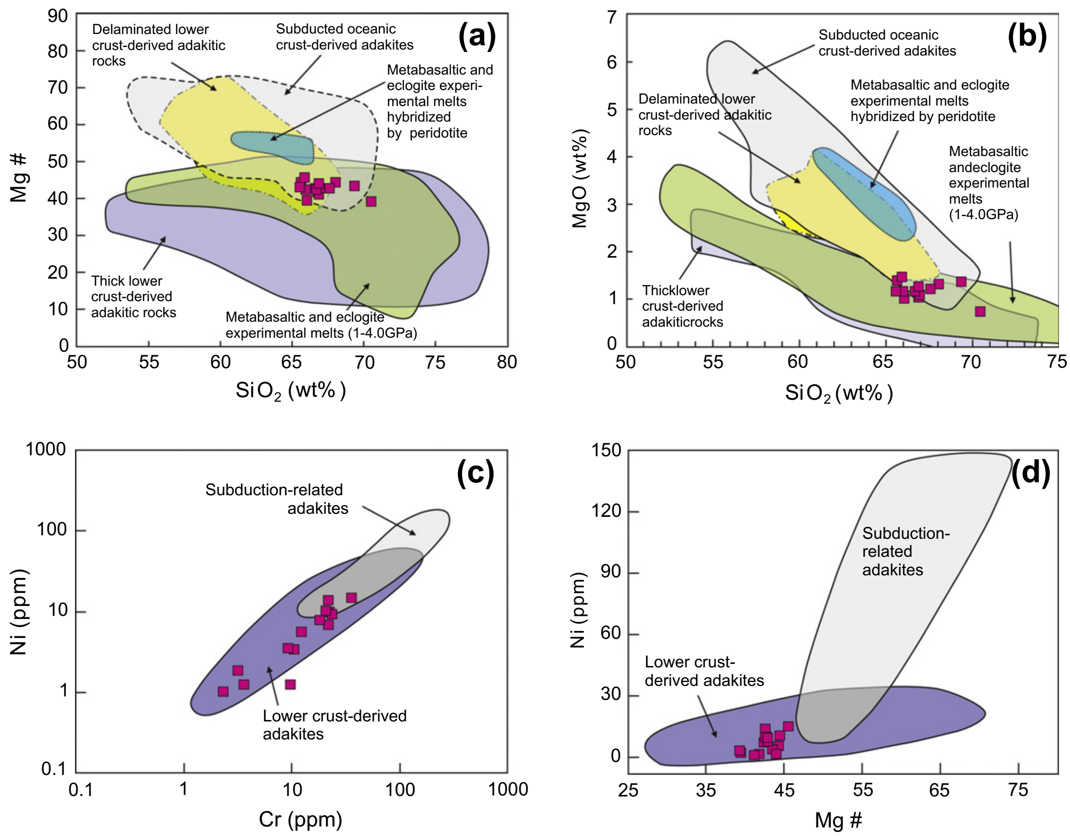

Fig. 12. Mg# (a) and MgO (b) versus SiO_2 and Ni versus Cr (c) and Mg# (d) diagrams for the adakite-like rocks in southern Anhui Province. Fields for different types of adakites and data sources are taken from Wang et al. (2006a,b).

attention has been paid to the characteristics and contributions of Neoproterozoic source materials in the existing models. Available geochemical data of the Mesozoic magmatic rocks does not reveal unambiguous arc-related volcanism in the interior of southern China, and the basaltic rocks of this age generally show enriched isotopic features that require an enriched mantle source, which decrease the possibility of a significant growth of juvenile crust from the depleted mantle that is expected from the subduction zone magmatism. Similar examples have been reported by Zheng et al. (2008) that concluded that the middle Neoproterozoic granitoids have been generated by the reworking of Early Neoproterozoic and Paleoproterozoic crust in the area, rather than representing the growth of juvenile crust.

The widespread Mesozoic granitoids in southern China (especially in the Cathaysia Block) and the associated basaltic rocks with enriched isotopic features probably suggest a widespread reworking event during Mesozoic time. The fact that some of the adakitic rocks occur in the eastern Jiangnan orogen may imply a close genetic relationship with the Proterozoic crust related to the Neoproterozoic orogeny between the Yangtze and Cathaysia Blocks. The Nd–Hf model ages of the adakite-like quartz porphyries are late Mesoproterozoic (Tables S7 and S8 in Appendix), consistent with that of many Neoproterozoic magmatic rocks (including the granitoids in southern Anhui Province and northwestern Jiangxi Province) in the eastern Jiangnan orogen. Therefore, the Neoproterozoic crustal materials formed during the assembly between the Yangtze and Cathaysia Blocks may be a dominant contribution to the source of the Mesozoic magmatic rocks.

The basaltic andesites, which were generated from the partial melting of an enriched lithospheric mantle, have a great deal of hornblende, suggesting their source was water-enriched. As discussed above, at least 6% water is needed. The high content of water implies that their source would have been metasomatized by fluids released from the dehydration of subducted oceanic crust, a hypothesis supported by the depletions of Nb, Ta and Ti relative to the LILE and REE and the low Zr and Hf contents (Fig. 8a). The remaining question is whether the metasomatism of the lithospheric mantle is the result of Mesozoic or Neoproterozoic subduction. As discussed above, if the lithospheric mantle was juvenile and metasomatized solely during Mesozoic time, melts sourced from it would not have relatively evolved isotopic characteristics of the basaltic andesites. The Caledonian-age orogeny was regarded as another Phanerozoic orogenic process in southern China with evident crust-scale deformation and metamorphism (Charvet et al., 1996; Li et al., 2010), although no mantle-derived rocks of this time have been reported so far. Instead, metasomatism of the lithospheric mantle must have occurred in Neoproterozoic time when the significant magmatic events took place around the Yangtze Block. The metasomatized lithospheric mantle (or the sub-arc mantle) was preserved until the Mesozoic because the water content and potential temperature in the mantle source was not enough to result in the partial melting of the mantle. In Mesozoic time, the subduction of Pacific Ocean Plate elevated the water contents in the preserved Neoproterozoic mantle and led to widespread mantle convection in the back-arc area. The large amount of water in the mantle source and the accompanying thermal disturbance from the upwelling of asthenospheric mantle then led to the partial melting of the "old" metasomatized lithospheric mantle. The underplating of the hydrous mafic magma may have led to the partial melting of lower portion of thick continental crust containing relicts of Neoproterozoic oceanic sediments, resulting in the formation of the studied adakite-like porphyries.

8. Conclusions

(1) The first case of adakite-like porphyries and associated mantle-derived basaltic andesites is reported in the eastern Jiangnan orogen, southern China. LA–ICP–MS U–Pb zircon dating suggests an age of 142 ± 1 Ma for these rocks.
(2) The basaltic andesites are enriched in hornblendes and have high anorthite contents (~80) in groundmass plagioclase, suggesting the high H_2O (~6 wt.%) contents for the magma source. They are depleted in Nb and Ta and were generated from the partial melting of enriched lithospheric mantle.
(3) The quartz porphyries show adakite-like geochemical features, with high Sr/Y and La/Yb ratios and low Y and Yb contents but low MgO, Ni, Cr contents. They may be directly generated from the partial melting of lower portion of continental crust, without interaction with the peridotite mantle. The mafic magma from the hydrous metasomatized lithospheric mantle led to the melting of thickened lower crust to form the adakite-like porphyries.
(4) The relatively low Sr contents and negative Eu negative anomalies of the porphyries suggest minor plagioclase as a residual mineral in the magma source, indicating the crust may be not such thick as suggested before. The new finding of Early Cretaceous adakite-like porphyry and associated mafic rocks in the eastern Jiangnan orogen implies a significant role of Neoproterozoic orogeny-related crust and related oceanic sediments in the formation of adakite-like rocks in Central-Eastern China.

Acknowledgements

This work was financially supported by the National Natural Science Foundation of China (No. 40730313), the 973 Program (Grant No. 2012CB416701), the Ministry of Land and Resources of China (No. 200811015), and the MiDeR, NJU (2008-III-01). The manuscript benefits greatly from the thoughtful and critical comments from three anonymous reviewers and the editor Louie. We thank Y.S. Liu for LA–ICP–MS U–Pb dating, M.Q. Zhang for major element analyses, T. Yang and H.Z. Wei for trace element analyses and H.J. Gong for CL imaging.

Appendix A. Supplementary material

Supplementary data associated with this article can be found, in the online version, at http://dx.doi.org/10.1016/j.jseaes.2012.10.017.

References

Atherton, M.P., Petford, N., 1993. Generation of sodium-rich magmas from newly underplated basaltic crust. Nature 362, 144–146.
Blatter, D.L., Carmichael, I.S.E., Deino, A.L., Rene, P.R., 2001. Neogene volcanism at the front of the central Mexican volcanic belt: basaltic andesites to dacites, with contemporaneous shoshonites and high-TiO_2 lava. GSA Bulletin 113, 1324–1342.
Bouvier, A., Vervoort, J.D., Patchett, P.J., 2008. The Lu–Hf and Sm–Nd isotopic composition of CHUR: constraints from unequilibrated chondrites and implications for the bulk composition of terrestrial planets. Earth and Planetary Science Letters 273, 48–57.
Castillo, P.R., 2006. An overview of adakite petrogenesis. Chinese Science Bulletin 51 (3), 257–268.
Charvet, J., Shu, L.S., Shi, Y.S., Guo, L.Z., Faure, M., 1996. The building of south China: collision of Yangzi and Cathaysia blocks, problems and tentative answers. Journal of Southeast Asian Earth Science 13, 223–235.
Chen, R., Zhou, J.C., 2001. Mineral chemistry and ^{40}Ar–^{39}Ar ages of hornblende gabbro from Tong'an, Fujian Province and their geological significance. Geological Review 47, 602–607 (in Chinese with English abstract).
Chen, C.-H., Lee, C.-Y., Shinjo, R., 2008. Was there Jurassic paleo-Pacific subduction in South China?: constraints from $^{40}Ar/^{39}Ar$ dating, elemental and Sr–Nd–Pb isotopic geochemistry of the Mesozoic basalts. Lithos 106, 83–92.
Chen, X.M., Chen, L.H., Xu, X.S., 2009. Study on the genesis of clinopyroxene megacrysts in the Cenozoic alkali basalt at Changle, Shandong Province. Acta Petrologica Sinica 25 (5), 1105–1116 (in Chinese with English abstract).
Chiaradia, M., 2009. Adakite-like magmas from fractional crystallization and melting-assimilation of mafic lower crust (Eocene Macuchi arc, Western Cordillera, Ecuador). Chemical Geology 265, 468–487.
Chung, S.-L., Liu, D.Y., Ji, J.Q., Chu, M.-F., Lee, H.-Y., Wen, D.-J., Lo, C.-H., Lee, T.-Y., Qian, Q., Zhang, Q., 2003. Adakites from continental collision zones: melting of thickened lower crust beneath southern Tibet. Geology 31 (11), 1021–1024.
Coldwell, B., Clemens, J., Petford, N., 2011. Deep crustal melting in the Peruvian Andes: Felsic magma generation during delamination and uplift. Lithos 125, 272–286.
Defant, M.J., Drummond, M.S., 1990. Derivation of some modern arc magmas by melting of young subducted lithosphere. Nature 347, 662–665.
Defant, M.J., Kepezhinskas, P., 2001. Evidence suggests slab melting in arc magmas. EOS (Transactions, American Geophysical Union) 82, 65–69.
Deng, J.H., Yang, X.Y., Sun, W.D., Yu, H., Chi, Y.Y., Yu, L.F., Zhang, Q.M., 2012. Petrology, geochemistry, and tectonic significance of Mesozoic shoshonitic volcanic rocks, Luzong volcanic basin, Eastern China. International Geology Review 54 (6), 714–736.
Drummond, M.S., Defant, M.J., Kepezhinskas, P.K., 1996. Petrogenesis of slab-derived trondhjemite–tonalite–dacite/adakite magmas. Transactions of the Royal Society of Edinburgh. Earth Sciences 87, 205–215.
Feeley, T.C., Hacker, M.D.X., 2006. Intracrustal derivation of Na-rich andesite and dacite magmas: an example from Volcan Ollage, Andean Central Volcanic Zone. Journal of Geology 103, 213–225.
Franzini, M., Leoni, L., Saitta, M., 1972. A simple method to valuate the matrix effect in X-ray fluorescence analysis. X-ray Spectrom 1, 151–154.
Gao, J., Klemd, R., Long, L.L., Xiong, X.M., Qian, Q., 2009. Adakitic signature formed by fractional crystallization: an interpretation for the Neo-Proterozoic meta-plagiogranites of the NE Jiangxi ophiolitic mélange belt, South China. Lithos 110, 277–293.
Ge, X.Y., Li, X.H., Chen, Z.G., Li, W.P., 2002. Geochemistry and petrogenesis of Jurassic high Sr/low Y granitoids in Eastern China: constrains on crustal thickness. Chinese Science Bulletin 47 (11), 962–968.
Goolaerts, A., Mattielli, N., de Jong, J., Weis, D., Scoates, J.S., 2004. Hf and Lu isotopic reference values for the zircon standard 91500 by MC–ICP–MS. Chemical Geology 206, 1–9.
Guo, F., Nakamuru, E., Fan, W., Kobayoshi, K., Li, C., 2007. Generation of Paleocene adakitic andesites by magma mixing; Yanji Area, NE China. Journal of Petrology 48, 661–692.
Hofmann, A.W., 2003. Sampling mantle heterogeneity through oceanic basalts: isotopes and trace elements. In: Carlson, R.W. (Ed.), The Mantle and Core. Treatise on Geochemistry. Elservier-Pergamon, Oxford, pp. 61–101.
Hou, Z.Q., Gao, Y.F., Qu, X.M., Rui, Z.Y., Moc, X.X., 2004. Origin of adakitic intrusives generated during mid-Miocene east–west extension in southern Tibet. Earth and Planetary Science Letters 220, 139–155.
Huang, F., Li, S., Dong, F., He, Y., Chen, F., 2008. High-Mg adakitic rocks in the Dabie orogen, central China: implication for foundering mechanism of lower crust. Chemical Geology 255, 1–13.
Jacobsen, S.B., Wasserburg, G.J., 1980. Sm-Nd isotopic evolution of chondrites. Earth and Planetary Science Letters 50 (1), 139–155.
Jiang, Y.H., Jiang, S.Y., Zhao, K.D., Ling, H.F., 2006. Petrogenesis of Late Jurassic Qianlishan granites and mafic dykes, Southeast China: implications for a back-arc extension setting. Geological Magazine 143 (4), 457–474.
JPIGS (Jiangxi Provincial Institute of Geological Survey), 2007. Regional Geological Survey Report (Jingdezhen Area, 1:250,000) (in Chinese with English Abstract).
Karsli, O., Dokuz, A., Uysal, I., Aydin, F., Kandemir, R., Wijbrans, J., 2010. Generation of the Early Cenozoic adakitic volcanism by partial melting of mafic lower crust, Eastern Turkey: implications for crustal thickening to delamination. Lithos 114, 109–120.
Kay, R.W., 1978. Aleutian magnesian andesites: melts from subducted Pacific Ocean crust. Journal of Volcanology and Geothermal Research 4, 117–132.
Kelemen, P.B., Hanghøj, K., 2004. One view of the geochemistry of subduction-related magmatic arcs, with an emphasis on primitive andesite and lower crust. In: Rudnick, R.L. (Ed.), The Crust: Treatise on Geochemistry, vol. 3. pp. 593–659.
Kuno, H., 1960. High-alumina basalt. Journal of Petrology 1, 12–145.
Li, W.X., Li, X.H., 2003. Adakitic granites within the NE Jiangxi ophiolites, South China: geochemical and Nd isotopic evidence. Precambrian Research 122, 29–44.
Li, Z.X., Li, X.H., 2007. Formation of the 1300-km-wide intracontinental orogen and postorogenic magmatic province in Mesozoic South China: a flat-slab subduction model. Geology 35, 179–182.
Li, S.G., Jagoutz, E., Lo, C.-H., Chen, Y., Li, Q., Xiao, Y., 1999. Sm/Nd, Rb/Sr, and 40Ar/39Ar isotopic systematics of the ultrahigh-pressure metamorphic rocks in the Dabie–Sulu Belt, central China: a retrospective view. International Geology Review 41, 1114–1124.
Li, X.H., Chen, Z.G., Liu, D.Y., Li, W.X., 2003. Jurassic gabbro–granite–syenite suites from Southern Jiangxi Province, SE China: age, origin, and tectonic significance. International Geology Review 45, 898–921.
Li, Z.X., Li, X.H., Wartho, J.A., Clark, C., Li, W.X., Zhang, C.L., Bao, C.M., 2010. Magmatic and metamorphic events during the early Paleozoic Wuyi–Yunkai orogeny, southeastern South China: new age constraints and pressure-temperature conditions. GSA Bulletin 122, 772–793.
Ling, M.-X., Wang, F.-Y., Ding, X., Hu, Y.H., Zhou, J.B., Zartman, R.E., Yang, X.Y., Sun, W.D., 2009. Cretaceous ridge subduction along the Lower Yangtze River Belt, Eastern China. Economic Geology 104, 303–321.

Ling, M.-X., Wang, F.-Y., Ding, X., Zhou, J.-B., Sun, W.D., 2011. Different origins of adakites from the Dabie Mountains and the Lower Yangtze River Belt, Eastern China: geochemical constraints. International Geology Review 53, 727–740.

Liu, Y.S., Gao, S., Yuan, H.L., Zhou, L., Liu, X.M., Wang, X.C., Hu, Z.C., Wang, L.S., 2004. U-Pb zircon ages and Nd, Sr, and Pb isotopes of lower crustal xenoliths from North China Craton: insights on evolution of lower continental crust. Chemical Geology 211, 87–109.

Liu, S., Hu, R.Z., Gao, S., Feng, C.X., Yu, B.B., Qi, Y.Q., Wang, T., Feng, G.Y., Coulson, I.M., 2009. Zircon U–Pb age, geochemistry and Sr–Nd–Pb isotopic compositions of adakitic volcanic rocks from Jiaodong, Shandong Province, Eastern China: constraints on petrogenesis and implications. Journal of Asian Earth Sciences 35, 445–458.

Liu, S.-A., Li, S.G., He, Y.S., Huang, F., 2010. Geochemical contrasts between early Cretaceous ore-bearing and ore-barren high-Mg adakites in Central-Eastern China: implications for petrogenesis and Cu–Au mineralization. Geochimica et Cosmochimica Acta 74, 7160–7178.

Liu, S., Hu, R.Z., Gao, S., Feng, C.X., Zhong, H., Qi, Y.Q., Wang, T., Feng, G.Y., Yang, Y.H., 2011. U-Pb zircon ages, geochemical and Sr–Nd–Pb isotopic constraints on the dating and origin of intrusive complexes in the Sulu orogen, Eastern China. International Geology Review 53 (1), 61–83.

Macpherson, C.G., Dreher, S.T., Thirlwall, M.F., 2006. Adakites without slab melting: high pressure differentiation of island arc magma, Mindanao, the Philippines. Earth and Planetary Science Letters 243, 581–593.

Maitre, R.W.L., Bateman, P., Dudek, A., Keller, J., Lemeyre, J., Bas, M.J.L., Sabine, P.A., Schmid, R., Sorensen, H., Streckeisen, A., Wooley, A.R., Zanettin, B., 1989. A Classification of Igneous Rocks and Glossary of Terms. Blackwell, Oxford.

Martin, 1999. Adakitic magmas: modern analogues of Archaean granitoids. Lithos 46, 411–429.

Moore, G., Carmichael, I.S.E., 1998. The hydrous phase equilibria (to 3 kbar) of an andesite and basaltic andesite from western Mexico: constraints on water content and conditions of phenocryst growth. Contributions to Mineralogy and Petrology 130, 304–319.

Moyen, J.-F., 2009. High Sr/Y and La/Yb ratios: the meaning of the "adakitic signature". Lithos 112, 556–574.

Newsom, H.E., White, W.M., Jochum, K.P., Hofmann, A.W., 1986. Siderophile and chalcophile element abundances in oceanic basalts, lead isotopic evolution and growth of the Earth's core. Earth and Planetary Science Letters 80, 299–313.

Niu, Y.L., 2005. Generation and evolution of basaltic magmas: some basic concepts and new views on the origin of Mesozoic–Cenozoic basaltic volcanism in Eastern China. Geological Journal of China Universities 11, 9–46.

Panjasawatwong, Y., Danyushevsky, L.V., Crawford, A.J., Harris, K.L., 1995. An experimental study of the effects of melt composition on plagioclase-melt equilibria at 5 and 10 kbar: implications for the origin of magmatic high-an plagioclase. Contribution to Mineralogy and Petrology 118, 420–432.

Peacock, S.M., Rushmer, T., Thompson, A.B., 1994. Partial melting of subducting oceanic crust. Earth and Planetary Science Letters 121, 227–244.

Pearce, N., Perkins, W., Westgate, J., Gorton, M., Jackson, S.E., Neal, C.R., Chenery, S., 1997. A compilation of published major and trace element data for NIST 610 and NIST 612 glass reference materials. Geostandard Newsletters 21, 115–144.

Prouteau, G., Scaillet, B., Pichavant, M., Maury, R.C., 2001. Evidence for mantle metasomatism by hydrous silicic melts derived from subducted oceanic crust. Nature 410, 197–200.

Pu, W., Gao, J.F., Zhao, K.D., Ling, H.F., Jiang, S.Y., 2005. Separation method of Rb–Sr, Sm–Nd using DCTA and HIBA. Journal of Nanjing University (Natural Sciences) 41 (4), 445–450 (in Chinese with English abstract).

Rapp, R.P., Watson, E.B., Miller, C.F., 1991. Partial melting of amphibolite/eclogite and the origin of Archean trondhjemites and tonalite. Precambrian Research 51, 1–25.

Richards, J.P., Spell, T., Rameh, E., Razique, A., Fletcher, T., 2012. High Sr/Y magmas reflect arc maturity, high magmatic water content, and porphyry Cu ± Mo ± Au potential: examples from the Tethyan arcs of central and eastern Iran and western Pakistan. Economic Geology 107, 295–332.

Rooney, T.O., Franceschi, P., Hall, C.M., 2011. Water-saturated magmas in the Panama Canal region: a precursor to adakite-like magma generation? Contribution to Mineralogy and Petrology 161, 373–388.

Seghedi, I., Bojar, A.-V., Downes, H., Rosu, E., Tonarini, S., Masson, P., 2007. Generation of normal and adakitelike calc-alkaline magmas in a non-subductional environment: an Sr–O–H isotopic study of the Apuseni Mountains Neogene magmatic province, Romania. Chemical Geology 245, 70–88.

Sisson, T.W., Grove, T.L., 1993. Experimental investigations of the role of H_2O in calc-alkaline differentiation and subduction zone magmatism. Contribution to Mineralogy and Petrology 113, 143–166.

Sisson, T.W., Grove, T.L., Coleman, D.S., 1996. Horblende gabbro sill complex at Onion Valley, California, and mixing origin for the Sierra Nevada batholith. Contribution to Mineralogy and Petrology 126, 81–108.

Söderlund, U., Patchett, P.J., Vervoort, J.D., Isachsen, C.E., 2004. The ^{176}Lu decay constant determined by Lu–Hf and U–Pb isotope systematics of Precambrian mafic intrusions. Earth and Planetary Science Letters 219, 311–324.

Stern, C.R., Killian, R., 1996. Role of the subducted slab, mantle wedge and continental crust in the genesis of adakites from the Andean Austral Volcanic Zone. Contributions to Mineralogy and Petrology 123, 263–281.

Stevenson, J.A., Daczko, N.R., Clarke, G.L., Pearson, N., Klepeis, K.A., 2005. Direct observation of adakite melts generated in the lower continental crust, Fiordland, New Zealand. Terra Nova 17, 73–79.

Sun, S.S., and McDonough, W.F., 1989. Chemical and isotopic systematics of oceanic basalt: implications for mantle composition and processes. In: Saunders, A.D., Norry, M.J. (Eds.), Magmatism in the Ocean Basins: Geological Society [London] Special Publications, vol. 42, pp. 313–345.

Sun, W.D., Xie, Z., Chen, J.F., Zhang, X., Chai, Z.F., Du, A.D., Zhao, J.S., Zhang, C.H., Zhou, T.F., 2003. Os–Os dating of copper and molybdenum deposits along the middle and lower reaches of the Yangtze River, China. Economic Geology and the Bulletin of the Society of Economic Geologists 98, 175–180.

Sun, W.D., Ding, X., Hu, Y.H., Li, X.H., 2007. The golden transformation of the cretaceous plate subduction in the west Pacific. Earth and Planetary Science Letters 262, 533–542.

Sun, W.D., Ling, M.X., Yang, X.Y., Fan, W.M., Ding, X., Liang, H.Y., 2010. Ridge subduction and porphyry copper gold mineralization: an overview. Science China – Earth Sciences 53, 475–484.

Sun, W.D., Zhang, H., Ling, M.X., Ding, X., Chung, S.L., Zhou, J., Yang, X.Y., Fan, W., 2011. The genetic association of adakites and Cu–Au ore deposits. International Geology Review 53, 691–703.

Tang, M., Wang, X.L., Xu, X.-S., Zhu, C., Cheng, T., Yu, Y., 2012. Neoproterozoic subducted materials in the generation of Mesozoic Luzong volcanic rocks: evidence from apatite geochemistry and Hf–Nd isotopic decoupling. Gondwana Research 21, 266–280.

Vervoort, J.D., Patchett, J.P., Albarede, F., Blichert-Toft, J., Rudnick, R., Downes, H., 2000. Hf–Nd isotopic evolution of the lower crust. Earth and Planetary Science Letters 181, 115–119.

Vervoort, J.D., Patchett, P.J., Soderlund, U., Baker, M., 2004. Isotopic composition of Yb and the determination of Lu concentrations and Lu/Hf ratios by isotopic dilution using MC–ICPMS. Geochemistry, Geophysics, Geosystems 5, 2004GC000721.

Wang, X.L., Zhou, J.C., Qiu, J.S., Gao, J.F., 2004. Geochemistry of the Meso- to Neoproterozoic basic-acid rocks from Hunan Province, South China: implications for the evolution of the western Jiangnan orogen. Precambrian Research 135, 79–103.

Wang, Q., Wyman, D.A., Xu, J.-F., Zhao, Z.H., Jian, P., Xiong, X.L., Bao, Z.W., Li, C.F., Bai, Z.-H., 2006a. Petrogenesis of Cretaceous adakitic and shoshonitic igneous rocks in the Luzong area, Anhui Province (Eastern China): implications for geodynamics and Cu–Au mineralization. Lithos 89, 424–446.

Wang, Q., Xu, J.-F., Jian, P., Bao, Z.W., Zhao, Z.H., Li, C.F., Xiong, X.L., Ma, J.L., 2006b. Petrogenesis of adakitic porphyries in an extensional tectonic setting, Dexing, South China: implications for the genesis of porphyry copper mineralization. Journal of Petrology 47, 119–144.

Wang, X.L., Zhou, J.C., Griffin, W.L., Wang, R.C., Qiu, J.S., O'Reilly, S.Y., Xu, X.S., Liu, X.M., Zhang, G.L., 2007. Detrital zircon geochronology of Precambrian basement sequences in the Jiangnan orogen: dating the assembly of the Yangtze and Cathaysia blocks. Precambrian Research 159 (1–2), 117–131.

Wang, Y.J., Fan, W.M., Cawood, P.A., Li, S.Z., 2008. Sr–Nd–Pb isotopic constraints on multiple mantle domains for Mesozoic mafic rocks beneath the South China Block hinterland. Lithos 106, 297–308.

Wang, X.L., Shu, L.S., Xing, G.F., Zhou, J.C., Tang, M., Shu, X.J., Qi, L., Hu, Y.-H., 2011. Post-orogenic extension in the eastern part of the Jiangnan Orogen: evidence from ca 800–760 Ma volcanic rocks. Precambrian Research. http://dx.doi.org/10.1016/j.precamres.2011.07.003.

Wang, G.G, Ni, P., Zhao, K.D., Wang, X.L., Liu, J.Q., Jiang, S.Y., Chen, H., 2012. Petrogenesis of the Middle Jurassic Yinshan volcanic-intrusive complex, SE China: implications for tectonic evolution and Cu-Au mineralization. Lithos. doi:http://dx.doi.org/10.1016/j.lithos.2012.05.030.

Wu, F.Y., Yang, Y.H., Xie, L.W., Yang, J.H., Xu, P., 2006a. Hf isotopic compositions of the standard zircons and baddeleyites used in U–Pb geochronology. Chemical Geology 234, 105–126.

Wu, R.X., Zheng, Y.F., Wu, Y.B., Zhao, Z.F., Zhang, S.B., Liu, X.M., Wu, F.Y., 2006b. Reworking of juvenile crust: element and isotope evidence from Neoproterozoic granodiorite in South China. Precambrian Research 146, 179–212.

Wu, J.Q., Tan, G.L., Zhang, B.T., Ling, H.F., Chen, P.R., 2011. Identification and genesis of the Early Cretaceous shoshonitic volcanic rock series in central Jiangxi Province. Geological Journal of China Universities 17 (4), 479–491 (in Chinese with English abstract).

Xie, G.Q., Mao, J.W., Li, X.W., Duan, C., Yao, L., 2011. Late Mesozoic bimodal volcanic rocks in the Jinniu basin, middle–lower Yangtze River Belt (YRB), East China: age, petrogenesis and tectonic implications. Lithos 127, 144–164.

Xiong, X.L., Li, X.H., Xu, J.F., Li, W.X., Zhao, Z.H., Wang, Q., Chen, X.M., 2003. Extremely high-Na adakitic-like magmas derived from alkali-rich basaltic underplate: the late Cretaceous Zhangtang andesites in the Huichang Basin, SE China. Geochemical Journal 37 (2), 233–252.

Xiong, X.L., Liu, X.C., Zhu, Z.M., Li, Y., Xiao, W.S., Song, M.S., Zhang, S., Wu, J.H., 2010. Adakitic rocks and destruction of the North China Craton: evidence from experimental petrology and geochemistry. Science in China (Earth Sciences) 54, 858–870. http://dx.doi.org/10.1007/s11430-010-4167-9.

Xu, J.-F., Shinjo, R., Defant, M.J., Wang, Q., Rapp, R.P., 2002. Origin of Mesozoic adakitc intrusive rocks in the Ningzhen area of east China: partial melting of delaminated lower continental crust? Geology 30, 1111–1114.

Xu, D.R., He, Z.L., Li, P.C., Chen, G.H., Xia, B., Fu, G.G., 2006. Discovery of the Late Yanshanian spilitic basalts in northeastern Hunan Province and its geological implications. Chinese Journal of Geology 41 (2), 311–332 (in Chinese with English abstract).

Xu, W.L., Hergt, J.M., Gao, S., Pei, F., Wang, W., Yang, D., 2008. Interaction of adakitic melt-peridotite: implications for the high Mg# signature of Mesozoic adakitic

rocks in the eastern North China Craton. Earth and Planetary Science Letters 265, 123–137.
Xu, H.J., Ma, C.Q., Zhang, J.F., Ye, K., 2012. Early Cretaceous low-Mg adakitic granites from the Dabie orogen, Eastern China: petrogenesis and implications for destruction of the over-thickened lower continental crust. Gondwana Research. http://dx.doi.org/10.1016/j.gr.2011.12.009.
Yan, D.-P., Zhou, M.-F., Zhao, D.G., Li, J.-W., Wang, G.H., Wang, C.-L., Qi, L., 2010. Origin, ascent and oblique emplacement of magmas in a thickened crust: an example from the Cretaceous Fangshan adakitic pluton, Beijing. Lithos 123, 102–120.
Zellmer, G.F., Iizuka, Y., Miyoshi, M., Tamura, Y., Tatsumi, Y., 2012. Lower crustal H_2O controls on the formation of adakitic melts. Geology. http://dx.doi.org/10.1130/G32912.1.
Zeng, L.S., Gao, L.-E., Xie, K.J., Jing, L.-Z., 2011. Mid-Eocene high Sr/Y granites in the Northern Himalayan Gneiss Domes: melting thickened lower continental crust. Earth and Planetary Science Letters 303, 251–266.
Zhang, Q., Wang, Y., Liu, H.T., Wang, Y.L., Li, Z.T., 2003. On the space-time distribution and geodynamic environments of adakites in China annex: controversies over differing opinions for adakites in China. Earth Science Fronties 10 (4), 385–400 (in Chinese with English abstract).
Zhang, L.J., Zhou, T.F., Yuan, F., Fan, Y., Cooke, D.R., 2011. Petrogenetic–metallogenetic setting and temporal–spatial framework of the Yueshan district. Anhui Province, East-Central China, International Geology Review 53 (5–6), 542–561.
Zheng, Y.-F., Fu, B., Gong, B., Li, L., 2003. Stable isotope geochemistry of ultrahigh pressure metamorphic rocks from the Dabie–Sulu orogen in China: implications for geodynamics and fluid regime. Earth Science Reviews 62, 105–161.
Zheng, Y.F., Wu, R.X., Wu, Y.B., Zhang, S.B., Yuan, H.L., Wu, F.Y., 2008. Rift melting of juvenile arc-derived crust: Geochemical evidence from Neoproterozoic volcanic and granitic rocks in the Jiangnan Orogen, South China. Precambrian Research 163, 351–383.
Zhou, X.M., Li, W.X., 2000. Origin of late Mesozoic igneous rocks of southeastern China: implications for lithosphere subduction and underplating of mafic magma. Tectonophysics 326, 269–287.
Zhou, X.M., Sun, T., Shen, W.Z., Shu, L.S., Niu, Y.L., 2006. Petrogenesis of Mesozoic granitoids and volcanic rocks in South China: a response to tectonic evolution. Episodes 29 (1), 26–33.
Zhou, Q., Jiang, Y.-H., Zhao, P., Liao, S.-Y., Jin, G, -D., 2012. Origin of the Dexing Cubearing porphyries, SE China: elemental and Sr–Nd–Pb–Hf isotopic constraints. International Geology Review 54 (5), 572–592.